



**HAL**  
open science

# The how and why of naphthalimide/heterocycle-fused hybrid dyes: an overview of the latest developments in the quest for dyes with innovative optical properties

Arnaud Chevalier

## ► To cite this version:

Arnaud Chevalier. The how and why of naphthalimide/heterocycle-fused hybrid dyes: an overview of the latest developments in the quest for dyes with innovative optical properties. *Organic & Biomolecular Chemistry*, In press, 10.1039/D3OB01035J . hal-04197458

**HAL Id: hal-04197458**

**<https://hal.science/hal-04197458v1>**

Submitted on 6 Sep 2023

**HAL** is a multi-disciplinary open access archive for the deposit and dissemination of scientific research documents, whether they are published or not. The documents may come from teaching and research institutions in France or abroad, or from public or private research centers.

L'archive ouverte pluridisciplinaire **HAL**, est destinée au dépôt et à la diffusion de documents scientifiques de niveau recherche, publiés ou non, émanant des établissements d'enseignement et de recherche français ou étrangers, des laboratoires publics ou privés.

# The how and why of naphthalimide/heterocycle-fused hybrid dyes: an overview of the latest developments in the quest for dyes with innovative optical properties.

Arnaud Chevalier\*<sup>a</sup>

In this review, a variety of hybrid structures fusing aromatic heterocycles of different natures to the Naphthalimide backbone are discussed. This strategy constitutes an efficient approach to generate original structures displaying singular photophysical properties and thus offering new perspectives in the fields of fluorogenic detection, optoelectronics, or photodynamic therapy. In this review, the different synthetic approaches and structures reported in the literature are discussed. A critical look at the design and the applications of these new fused hybrids allows to evaluate the benefits and drawbacks of fused hybrid strategy applied to Naphthalimides.

## Introduction

Of the numerous fluorophores commonly used for optical imaging applications, 4-amino-naphthalimide (ANI) has encountered great success in recent years. Its optical properties characterized by a green emission, combined to a large Stokes shift, allow its use in a cellular environment. Thanks to high chemical stability, a large number of analogs have been developed to date using multiple reaction conditions.<sup>1</sup>

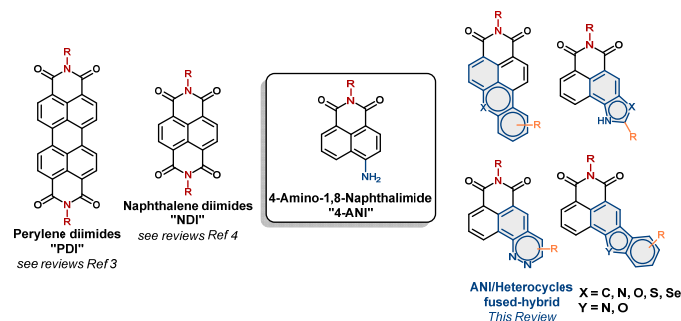


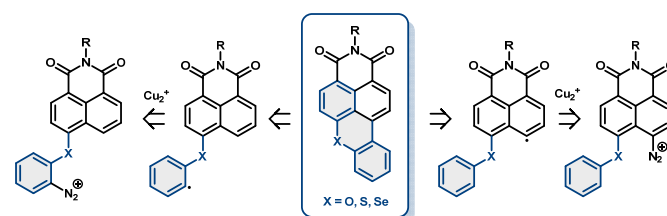
**Figure 1.** Structure of 4-Amino-1,8-Naphthalimide “4-ANI” and fused hybrid including Perylene diimide “PDI”, Naphthalene diimides “NDI” and general structures of ANI/heterocycles fused hybrid dyes.

The main asset of this fluorophore is undoubtedly its fluorogenic nitrogen atom which has been used to make a large number of fluorogenic sensors intended to detect a wide variety of analytes.<sup>2</sup> ANI is thus one of the most used aniline fluorophores in this field. Its main limitation is probably a green emission, also a bathochromatic shift of the absorption and emission wavelengths would allow providing more efficient tools for optical imaging. This is why several derivatizations of this scaffold have been attempted, in particular by fusing the naphthalimide ring with aromatic moieties, leading to fluorophores with innovative properties. Perylene diimides (PDIs) and Naphthalene Diimides (NDIs) are the most illustrative example constituting a kind of phenyl-fused dimers of naphthalimide. Several good reviews have been published

focusing on the contributions PDIs<sup>3</sup> and NDIs<sup>4</sup> so they won't be discussed here. In this review, we will focus on hybrid fluorophores that have arisen from the fusion between naphthalimides and other aromatic heterocycles. We will expose the representative examples reported in the literature, their structural diversity, and the synthetic strategies employed to obtain them. We will also provide an overview of the contribution afforded by these modifications to the optical properties by presenting applications that resulted from it.

## Heteroxanthene fused Dyes

To start this tour of fused hybrids, we present the molecules incorporating a xanthene or heteroxanthene motif.



**Scheme 1.** Synthetic approach to access xanthene and heteroxanthene fused hybrid dyes.

These molecules have been known for several decades and are most frequently obtained from either 5-(2-aminoheteroaryl) or 4-amino-5-heteroaryl 1,8-naphthalimide derivatives and Pschorr cyclization (Scheme 1). This intra-molecular cyclization of 2-substituted anilines, discovered in the 19th century, occurs *via* their conversion into diazonium salts.<sup>5</sup> The action of metallic copper causes the homolytic rupture of the C-N<sub>2</sub><sup>+</sup> bond and the consequent formation of an aryl radical together with the release of N<sub>2</sub>. This radical then initiates a cyclization to provide the hetero-xanthene polycycle. It is the nature of the atom X (Scheme 1) that will determine the nature of the hetero xanthene.

**Hétérothioxanthenes (X = S), the historic dye.**

Thioxanthene fused hybrid of naphthalimide is one of the oldest examples presented in the literature. This is the component of the Hostoal Yellow or Solvent yellow pigment used to color solvents. More recently its good solubility in organic solvents and low solubility in aqueous medium have been exploited for the observation of lipid droplets.<sup>6</sup>

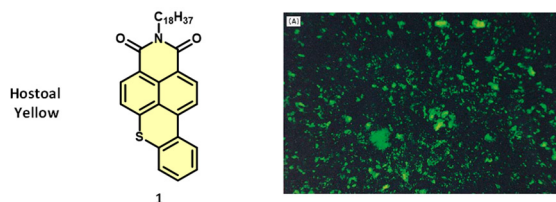
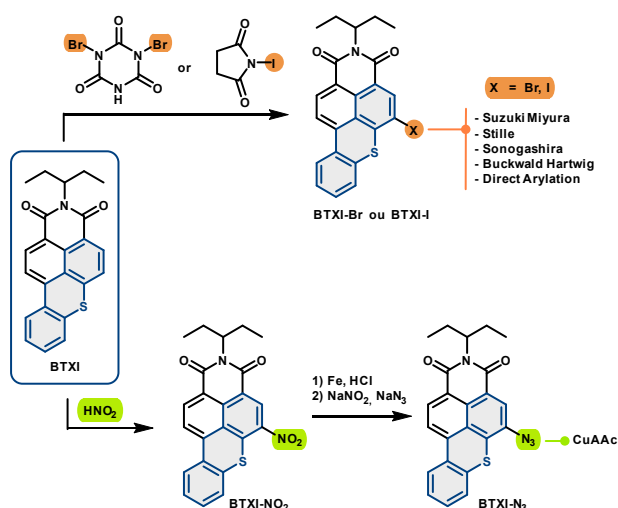


**Figure 2.** Hostoal Yellow, a pigment used to color solvents and for fluorescent observation porous ceramics after impregnation. Figure adapted from the literature.<sup>7</sup> Copyright 2003 John Wiley & Sons, Inc

Its green fluorescence emission was also used in 1996 to visualize the pores of ceramics by impregnating epoxy resins (figure 2).<sup>7</sup> Photophysical properties of these fluorophores can be modulated with post-synthetic functionalization. In this context, C. Cabanetos et al described methods for the efficient regioselective halogenation<sup>8</sup> or nitration<sup>9</sup> on thioxanthene scaffold (BTXI) as presented in Scheme 2.



**Scheme 2.** Nitro and halogen derivatives of thioxanthene/naphthalimide fused hybrids to offer multiple perspective of post-functionalization.<sup>8-9</sup>

These transformations provide access to new intermediates that can be introduced in multiple palladocatalyzed coupling reactions (Suzuki Miyaura, Stille, Sonogashira Buchwald etc...)<sup>8</sup> or in copper catalysed click reactions to expand the scope of chemical modification.<sup>9</sup> The practical application of this chemistry led to multiple analogs of Thioxanthenes. Among them, dimers were obtained by copper-catalyzed Aryl-Aryl bond formation. The authors report a significant decrease in fluorescence of these compounds in solution, probably due to a tendency to move towards a non-emissive triplet state by intersystem crossing. On the other hand, they mention a significant fluorescence in the solid state.<sup>10</sup> These properties have been used to produce OLEDs represented in Figure 3a, with emission colors ranging from blue to orange. This work testified to the utility of fused thioxanthene/ANI hybrids in the

field of optoelectronics. Among the multiple contributions in the chemistry of this family of dyes,<sup>11</sup> the same group recently obtained thiochromenocarbazole derivatives with new electroluminescent properties which could be used for the fabrication of flexible OLED materials (Figure 3b).<sup>12</sup>

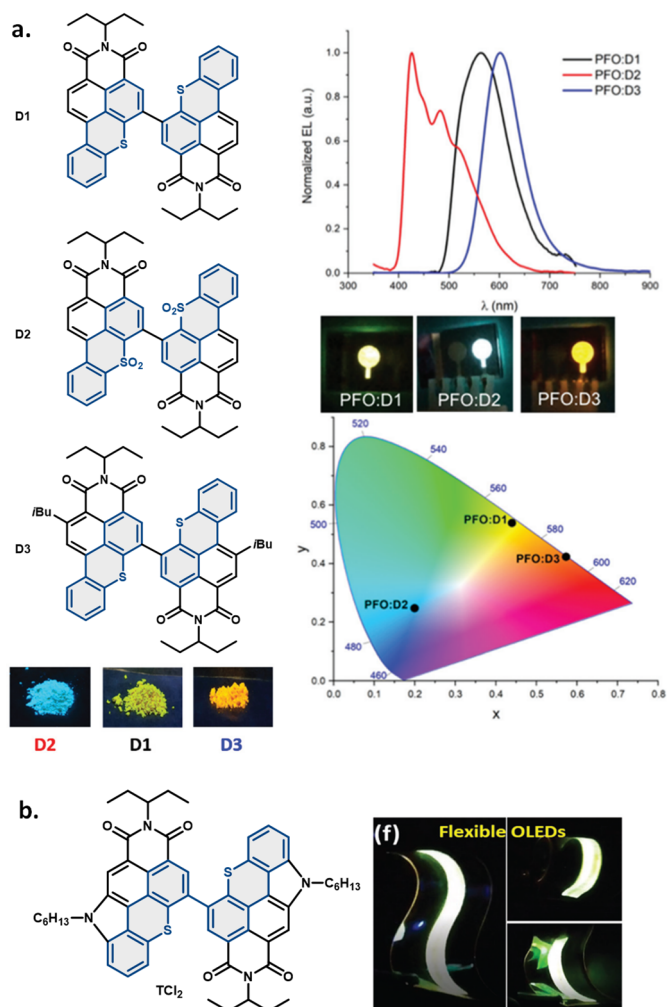


**Figure 3.** Aryl-aryl bond formation to provide dimers of thioxanthene/naphthalimide fused hybrids as potent OLEDs. a. structures of dimers D1, D2 and D3 and photography of the powder under white light, electroluminescence spectra and CIE color coordinate spectra. Figures adapted from the literature.<sup>10</sup> b. Structure of thiochromenocarbazole imide TCl<sub>2</sub> and photography of flexible OLED. Figures adapted from the literature.<sup>12</sup>

In 2016, Qian's group used the thioxanthene ring as the central element of a fused naphthalimide dimer presented in Figure 4.<sup>13</sup> These dimers exhibit a significant bathochromic shift of the emission wavelength reaching about 600 nm, which is close to red thus constituting a major asset for optical imaging in cellular environment. On the other hand, the fluorescence efficiency in solution is very weak and the quantum yields reach painfully 1%.

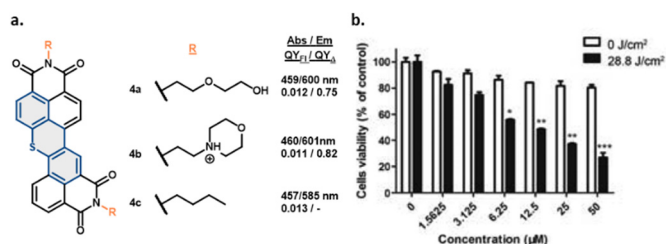
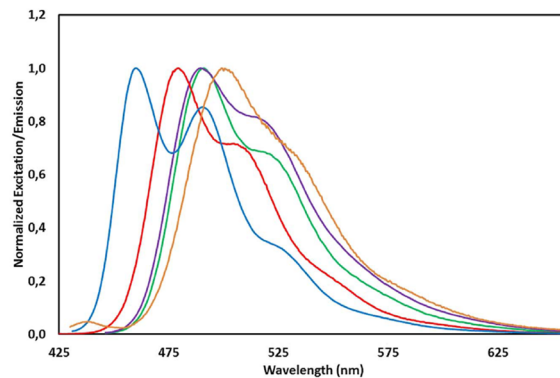
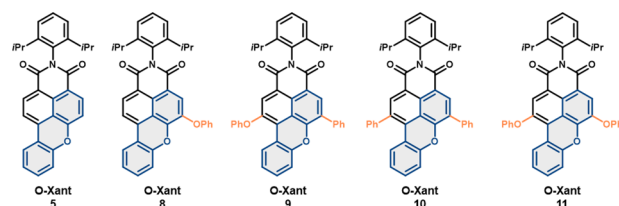


**Figure 4.** a. Structure and use of thioxanthene/naphthalimide fused hybrids for PDT applications. b. MTT assays of **4a** exposed with laser irradiation of 0 and 28.8 J/cm<sup>2</sup> in MKN45 cells. Figures adapted from the literature.<sup>13</sup> Reprinted (adapted) with permission from L. Zhang, Z. Huang, D. Dai, Y. Xiao, K. Lei, S. Tan, J. Cheng, Y. Xu, J. Liu and X. Qian, *Org. Lett.*, **2016**, 18, 5664. Copyright 2016. American Chemical Society

Theoretical calculations showed a low energy gap between the singlet excited state and the triplet state making the switch from one to the other possible by intersystem crossing (ISC). This result, which explains the low fluorescence efficiency in solution, led the authors to evaluate these molecules for use in photodynamic therapy (PDT). This was confirmed by an increase in their toxicity after light irradiation. More recently, Cabanetos's group showed that thionation of such benzoenzothioxanthene imide favors the triplet state, leading to chromophores that exhibited remarkable phototherapeutic activity in HeLa cells.<sup>14</sup> This example comes to complete a set of data from the literature, which tend to consider a facilitated passage to the triplet state for the fused thioxanthene derivatives. As a consequence, their use for optical imaging seems to be compromised. On the other hand, it opens perspectives in optoelectronics and photodynamic therapy.

#### Underexplored oxoxanthenes/ANI hybrids (X = O)

To our knowledge, the first example fused ANI-Xanthene hybrid dye was obtained and published by Peters and Behesti in 1989, and uses a synthesis strategy involving a Pischorr cyclization.<sup>15</sup> Absorbance properties were found quite similar to those of the naphthalimide 4-ANI with an absorption maximum centered near 425 nm in chlorobenzene. This family of compounds has for a long time been considered mainly for therapeutic applications, especially antitumor activity in a hypoxic environment.<sup>16</sup> It is only very recently, in 2018, that the luminescence properties of these compounds have been explored. Lub et al. showed that the addition of phenyl or phenoxy groups to the xanthene moiety led to compounds endowed with high photoluminescence efficiency (PLQE measured between 0.92 and 0.96) over an emission range of 450 nm to 520 nm (Figure 5).<sup>17</sup> They also exhibit a lifetime beyond 10 000 hours, measured for 10% bleaching after excitation at 450 nm (blue light) in a PET matrix.



PLQE and lifetime of organic yellow emitting molecules in a PET matrix (in hours) after 10% bleaching at an exposure of 0.016 W/cm<sup>2</sup> blue (450 nm) at 60 °C in air.

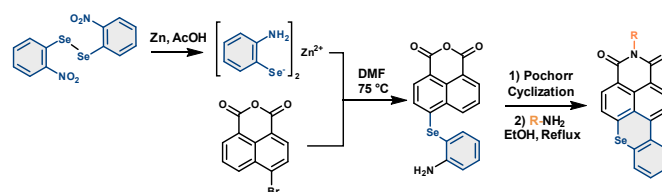
Compound	5	8	9	10	11
PLQE	0.93	0.95	0.92	0.92	0.92
Lifetime (h)	2800	12000	14000	27000	12000

**Figure 5.** Structures of Xanthene/Naphthalimide fused hybrids dyes and their fluorescent properties. Emission spectra of compounds **O-Xant5** (blue line), **O-Xant8** (red line), **O-Xant10** (purple line), **O-Xant9** (green line), and **O-Xant11** (brown line) were recorded in ethyl acetate. Figures adapted from the literature.<sup>17</sup> Reprinted from Dyes and Pigments, Vol 149, Johan Lub, Sylvain L.J. Hamon, Paul A. van Hal, Ton J. Visser, Jan M. Jansen, Rifat A.M. Hikmet, Synthesis of yellow fluorescent dyes derived from benzoxanthene that can be used in colour converters for remote phosphor LED systems. Pages No.662-668, Copyright (2018), with permission from Elsevier.

These new Xanthene/ANI fused hybrids constitute serious candidates for blue to yellow color converters due to their high photoluminescence quantum yield and photostability.

#### Selenoxanthenes (X = Se) as antiviral agents.

A divergent synthetic strategy for the synthesis of multiple selenoxanthene/ANI fused hybrids with different substituents on the imide nitrogen has recently been reported. (Scheme 3).<sup>18</sup>



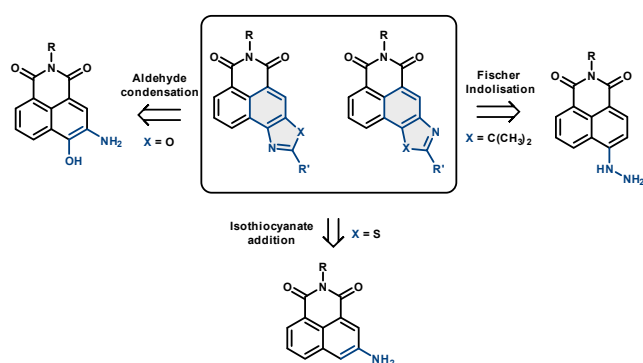
**Scheme 3.** Synthetic pathway to selenoxanthene/ANI fused hybrid dyes.<sup>18</sup>

These molecules can regulate the expression of the TMPRSS2 gene by stabilizing G-quadruplex. This significantly inhibits the growth and propagation of the HIV virus in vitro, and according to the authors may constitute a new anti-influenza strategy. Unfortunately, no photophysical study was reported for these compounds. This new example confirms that to date, the use of heteroxanthene/ANI fused hybrid molecules are mostly considered for therapeutic applications, also examples from the

literature tend to assert that they are good candidate for bioelectronics applications.<sup>10,12</sup>

For all the examples presented above, one can wonder what would be the impact on fluorescence of introducing an electron donating group (EDG) in a judiciously selected position of xanthenone or heteroxanthenone/ANI fused hybrids, to allow the establishment of an internal charge transfer (ICT) between this EDG and the phthalimide unit electron-withdrawing group (EWG). I believe that this is a plausible and relevant way of reflection in the quest for fluorescent chromophores fusing an ANI backbone to a xanthenone or heteroxanthenone unit.

### Benzimidazoles, benzothiazoles, benzoxazoles, and indoles hybrids offer new perspectives for fluorescence in biological media



**Scheme 4.** Retrosynthetic access to benzothiazoles, benzoxazoles, and indoles fused hybrid dyes.

The way to synthesize these hybrids depends largely on the nature of the heterocycle to be formed. For example, Fisher's indolization conducted on hydrazine derivatives of naphthalimides is favored to give access to indole/naphthalimide hybrids (Scheme 4). On the other hand, the preparation of benzoxazole usually relies on condensation reactions of aldehydes on *ortho* hydroxy anilines, whereas benzothiazoles can be obtained using isothiocyanates.

### Indole-fused naphthalimides as powerful building blocks for merocyanine- and cyanine-fused ANIs

In 2013, Zhang's group describes the preparation of naphthalimide/Indoles hybrids from hydrazine derivatives of naphthalimide and Fischer indolization.<sup>19</sup> The use of 3-methyl-2-butanone for this reaction allows access to the **L0** hybrid exhibiting disappointing fluorescence properties with a marked hypsochromic shift although the fluorescence quantum yield is rather good. On the other hand, the analogs obtained by indole reduction, **L1**, and **L2** hybrids show much more interesting emission properties including a clear bathochromic shift. Although devoid of interesting photophysical characteristics the Indole **L0** hybrid is a well-known precursor for the elaboration of  $\pi$ -extended fluorophores such as cyanines or merocyanines. Thus, Weiyang Lin's group proposed to use it in Knoevenagel reactions with aldehydes of various natures (Figure 6).<sup>20</sup> In this way, merocyanine derivatives were obtained with particularly relevant properties for biological purposes. Indeed, the **TPFC-5** shows a far-red emission measured at 669 nm with a fluorescence quantum yield of 0.105 in PBS buffer (Figure 6c).

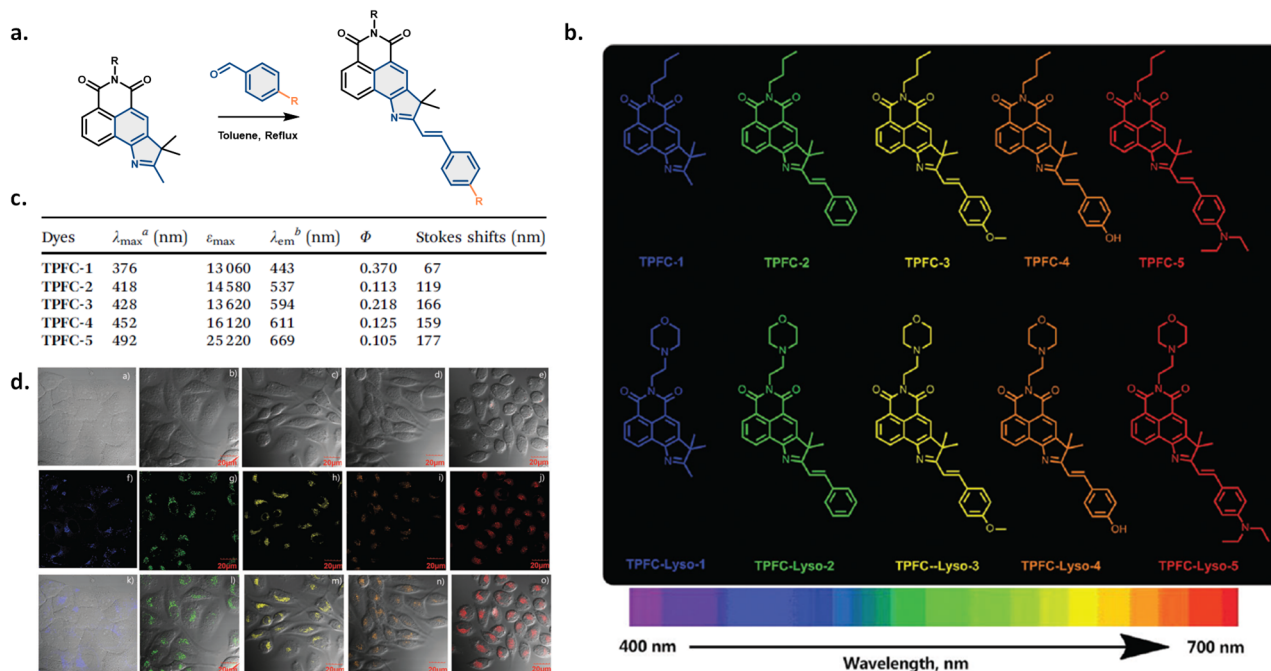


**Figure 6.** a. Synthesis of merocyanine dyes from Indole/Naphthalimide fused hybrid molecules. b. Structures of multiple analogs covering the emission spectrum from 400 nm to 700 nm. c. Photophysical properties of TPFC dyes. d. Two-photon imaging of lysosome with TPFC-Lyso dyes. Figure generated by combining multiples figure of the original article.<sup>20</sup>

Moreover, these compounds can be excited at two photons allowing the multicolor imaging of brain slices of mice. The nitrogen of the phthalimide motif can be functionalized by adding a morpholine unit leading to efficient two-photon lysosomal markers (Figure 6d). This example shows clearly how indole, despite its disappointing photophysical properties, can be used to make much more sophisticated fluorophores that have demonstrated real utility for optical imaging. Inspired by this work, multiple studies have since proposed to use these fluorophores as starting bases for the design of fluorogenic probes. This way, two OFF-ON red-emitting probes were published by Song's group (Figure 7a).

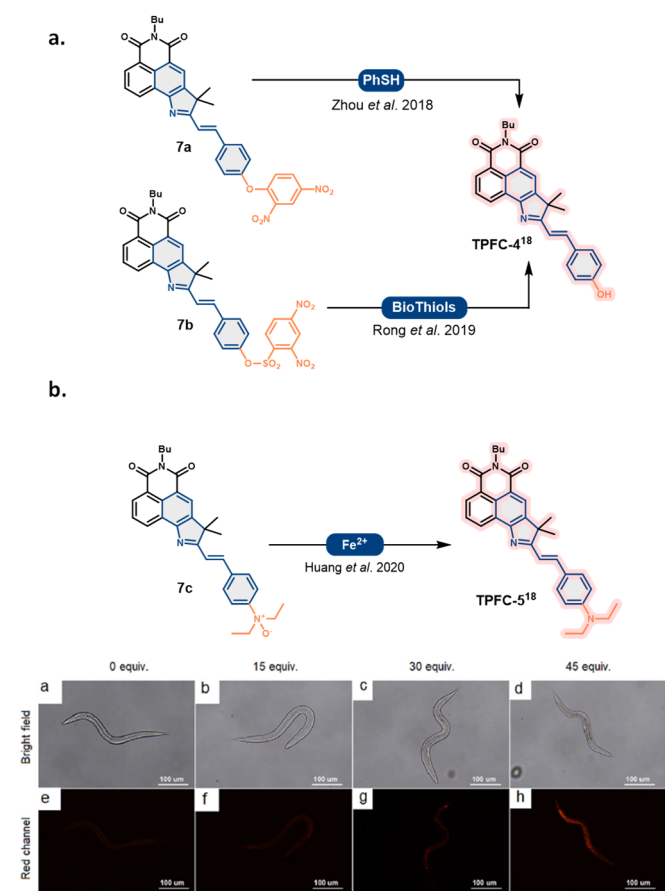


**Figure 7.** a. Examples of fluorogenic probes derive from phenolic nercyanines/naphthalimide fused hybrid dyes **TPFC-4** for detection of thiols. b. Principle of the fluorogenic detection of  $\text{Fe}^{2+}$  with N-oxide analog of diethylamino merocyanines/naphthalimide fused hybrid dye **TPFC-5** and application *in vivo* in *C. elegans* model. Figures adapted from the literature.<sup>21</sup> Reprinted from Chinese Chemical Letters, Vol 31, Lina Huang, Yu Chen, Yuqiang Zhao, Yumin Wang, Junwei Xiong, Junfeng Zhang, Xianghua Wu, Ying Zhou, A ratiometric near-infrared naphthalimide-based fluorescent probe with high sensitivity for detecting  $\text{Fe}^{2+}$  *in vivo* Pages No.2941-2944, Copyright (220), with permission from Elsevier.

The probe **7a** was dedicated to the sensing of thiophenol<sup>22</sup> whereas **7b** proved to be efficient to detect other biothiols such as glutathione or cystein.<sup>23</sup> By oxidizing the fluorophore **TPFC-5**, Huang and coworkers obtained the probe **7c** which turned out to be an efficient OFF-ON sensor for  $\text{Fe}^{2+}$  ions, even *in vivo* in *C. elegans* model (Figure 7b).<sup>21</sup> More recently, Xuhong Qian's

group has described the first cyanine based on fused ANI/Indole hybrids.<sup>24</sup> They have demonstrated that it is possible to alkylate fused ANI/Indoles hybrids by opening the propane sultone. The resulting indolinium was engaged under conditions commonly used for the preparation of Cy7 cyanines, which provided the compound **ML880** (Figure 8). This new fluorophore showed very singular photophysical properties with an absorption maximum centered around 860 nm and emitting between 880 and 912 nm depending on the solvents used. This particularly marked redshift is due to a strong electron delocalization demonstrated by a series of DFT and TD-DFT calculations. The fluorescence quantum yields reach about 10% in the studied organic solvents, while no fluorescence is observed in a PBS buffer despite good solubility. This led the authors to consider the possibility of a non-radiative de-excitation or a passage to a non-radiative triplet state as an explanation for these results.

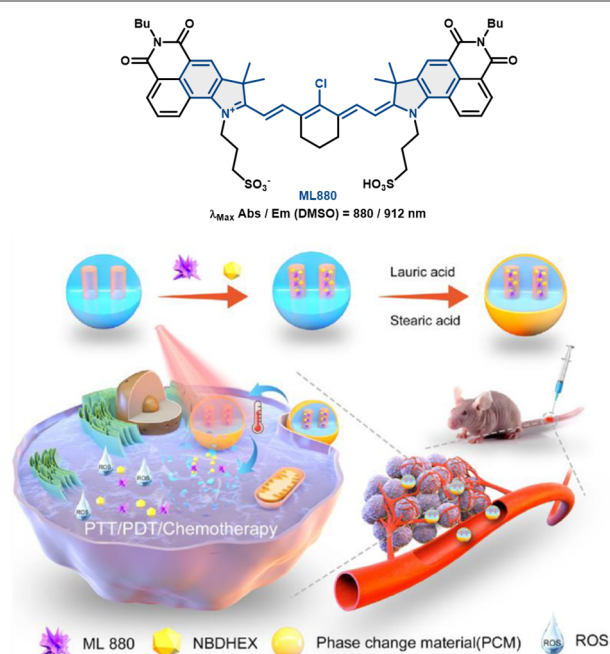
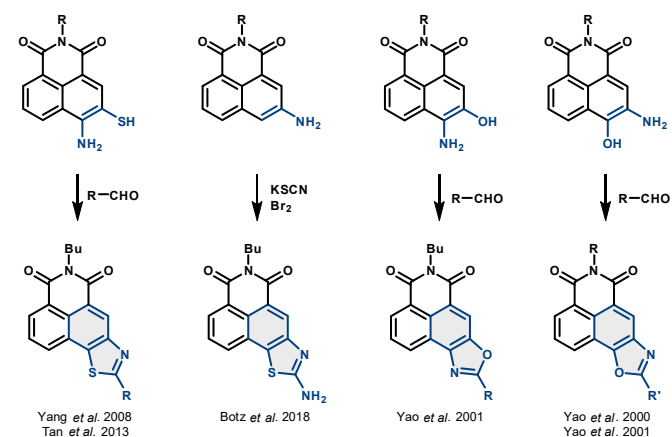


**Figure 8.** Structure and schematic representation of ML 880 Cyanine/ANI fused hybrid dye's therapeutic function. NBDHEX stands for 6-(7-nitro-2,1,3-benzoxadiazol-4-ylthio)hexanol. Figure adapted from the literature<sup>24</sup>

These hypotheses were verified during photodynamic and photothermal therapy studies which showed good activity of **ML880** first on a HepG2 cell model. Following these observations, the authors have prepared mesoporous organosilica nanocarriers loaded with the dye ML880 and NBDHEX (a specific inhibitor of Glutathione-S-transferase) to allow a synergistic PDT/PTT/chemotherapy effect on a living mouse model bearing a liver tumor. These results constitute a new example that attests to the utility of Naphthalimide/Indole hybrids. Although they have limited photophysical properties, they are useful building blocks for access to more sophisticated and efficient compounds, both in imaging and for cancer therapy applications.

### Benzoxazole and benzothiazoles maybe misestimated molecules

The extension of the conjugation by a 5-membered heterocycle ring has also been implemented for hybrid derivatives incorporating benzothiazole and benzoxazole units. The synthesis of benzoxazoles resorts exclusively to the use of *ortho* hydroxyaniline in a condensation reaction with aldehydes (Scheme 5).



**Scheme 5.** Synthetic accesses to benzoxazoles and benzothiazoles/naphthalimide fused hybrid dyes.

It is principally Qian's group who developed this chemistry at the beginning of the 2000's.<sup>25</sup> The photophysical properties of these compounds have not been investigated, the main objective here is to utilize the compounds for therapeutic purposes, in particular as DNA cleavers. Although benzothiazole

derivatives can be accessed by condensation of aldehyde on *ortho* thioaniline. Then, 2-amino-benzothiazole analogs were obtained by Qian et al.<sup>26</sup> and then Gateau et al using the reaction of 3-amino-1,8-naphthalimide derivatives with potassium cyanogen generated *in situ* from potassium isothiocyanate and bromine.<sup>27</sup> This time again, only a few data are available on the photophysical properties and their use appears to be restricted to applications as DNA cleavers.

### Imidazoles/ANI fused hybrids fluorophores, from in situ formation to OR logic-gate sensor

Benzimidazoles are also heterocycles that can be fused to naphthalimides. Song's group first explored the possibility of forming *in situ* a blue-emitting benzimidazolone **9'a** unit by reaction of a non-fluorescent *ortho*-dianiline naphthalimide **9a** with phosgene (Figure 9a). This concept has proven effective in detecting triphosgene but also diphosgene at particularly low concentrations (ppm level).<sup>28</sup> Along the same lines, Zheng's group used a dianiline unit **9b** that reacts with formaldehyde to yield a benzimidazole unit **9'b** presented in Figure 9b.<sup>29</sup> In this case the green emission allows the detection of formaldehyde on L929 cells with a micromolar concentration of probe. Such formation of the fluorophore by the reaction of compounds carrying an *ortho* dianiline motif with endogenous stimulus has already been reported for other classes of fluorophores.<sup>30</sup> Song's group has recently extended this concept to the derivation of 2-benzimidazol-2-yl aniline motif fused to naphthalimide, taking advantage of the nucleophilicity of the benzimidazole nitrogen.<sup>31</sup>

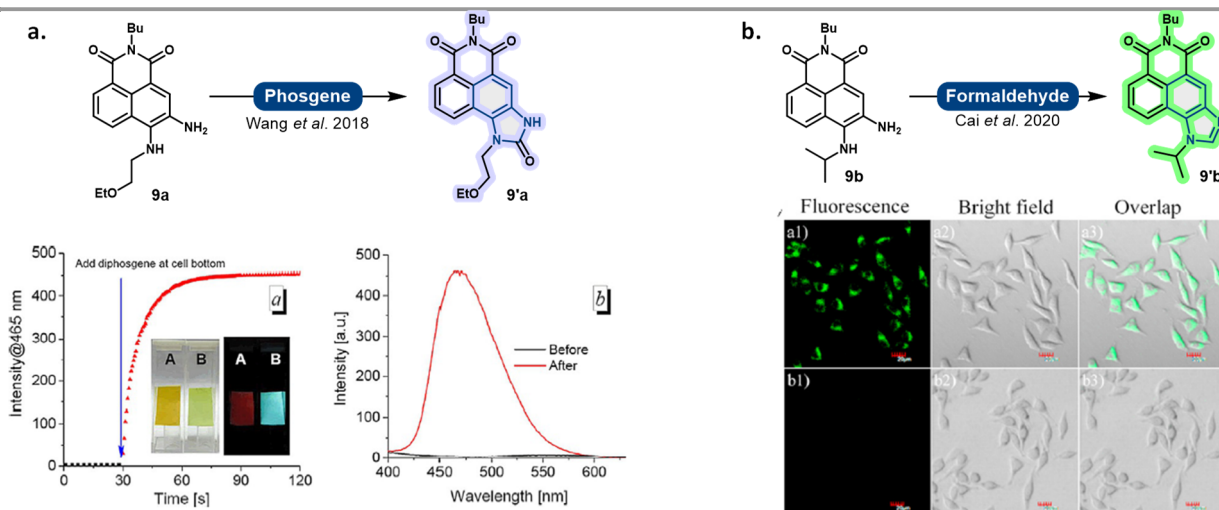


**Figure 9.** a. Fluorogenic detection of phosgene by *in situ* formation of imidazolone/naphthalimide fused hybrid blue emitting dye. Figure adapted from literature<sup>28</sup> © 2018 Wiley-VCH Verlag GmbH & Co. KGaA, Weinheim b. Fluorogenic detection of formaldehyde by *in situ* formation of green emitting imidazole/naphthalimide fused hybrid dye. Figure adapted from literature.<sup>29</sup> Reprinted from Tetrahedron, Vol 76/45, Songtao Cai, Chang Liu, Xiaojie Jiao, Liancheng Zhao, Xianshun Zeng, A rational design of fluorescent probes for specific detection and imaging of endogenous formaldehyde in living cells, Pages No. 131617, Copyright (2020), with permission from Elsevier.

With such a strategy, they designed a fluorogenic sensor **10a** for discrimination between phosgene and triphosgene (Figure 10). The aniline function of the probe could first react with both phosgene and triphosgene, yielding the corresponding carbamoyl chloride **10b** and trichloromethyl carbamate **10c** respectively. While the latter doesn't evolve more and exhibits blue emission, the carbamoyl chloride intermediate can react

with benzimidazol nitrogen leading to the green emitting quinazoline-2-one **10d**. This way, with a single discriminating probe, the authors have demonstrated that they can differentiate phosgene from triphosgene in a fluorogenic OR logic gate<sup>32</sup> approach which is also very sensitive (LOD 3.2 nM).

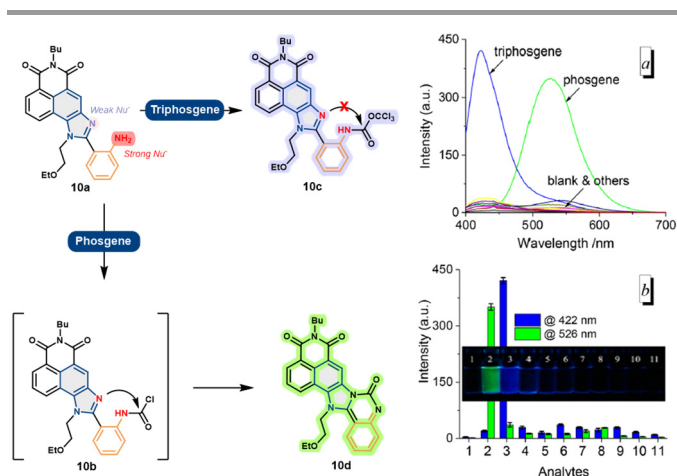
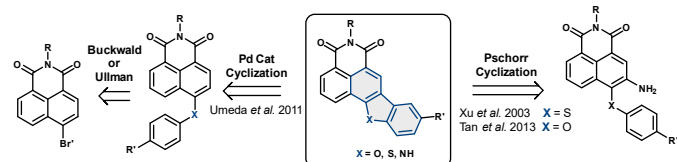


**Figure 10.** Schematic representation of "OR" logic-gate principle applied to the detection of phosgene or triphosgene with an imidazole/naphthalimide fused hybrid based probe. (a) Fluorescence spectra were recorded after activation of **10a** with multiple stimuli. (b) Fluorescence intensity at 422 (blue column)/526 nm (green column) of **10a** (10  $\mu$ M) before (1) and after additions of (2) phosgene (30  $\mu$ M), (3) triphosgene (20  $\mu$ M), and other analytes (50  $\mu$ M) in 1,4-dioxane after 4 min. (4)  $(\text{COCl})_2$ , (5)  $\text{SOCl}_2$ , (6)  $\text{SO}_2\text{Cl}_2$ , (7)  $\text{POCl}_3$ , (8)  $\text{NO}$ , (9)  $\text{HCl}$ , (10)  $\text{DCP}$ , (11)  $\text{DCNP}$ ,  $\lambda_{\text{ex}} = 390$  nm. (Inset) Photograph of above solutions under 365 nm light. Adapted from the literature.<sup>31</sup> Reprinted (adapted) with permission from S. L. Wang, C. Li and Q. H. Song, *Anal. Chem.*, **2019**, *91*, 5690. Copyright 2019, American Chemical Society

In this part, We have seen multiple examples of molecules, mainly with therapeutic applications (especially benzothiazole and benzoxazole/ANI fused hybrid dyes). Nonetheless, the representative examples use indole derivatives as building blocks for the construction of fluorophores with particularly interesting properties. This leads us to suggest that the main interest of these hybrids may not lie in their intrinsic photophysical properties, but rather in their potential use for the elaboration of more sophisticated fluorophores such as cyanines or merocyanines dyes. We can therefore expect that the use of hybrids associating benzothiazoles, oxazoles, or benzimidazoles skeletons to the naphthalimide motif should be considered for the construction of new fluorophores of merocyanine or cyanine family. This could open new perspectives as it has been demonstrated with the use of Indoles/ANI fused derivatives.

## Dibenzofuran, carbazoles and dibenzothiophenes

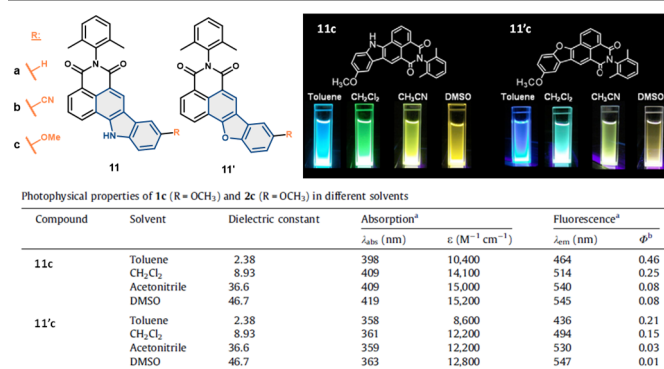
Fusing a dibenzofuran, carbazole or dibenzothiophene heterocycle requires the formation of a C-C bond (Aryl-Aryl) by intramolecular cyclization as presented in Scheme 6.



**Scheme 6.** Retrosynthetic accesses to dibenzofuran, dibenzothiophene and carbazole based hybrid dyes.

This has been undertaken using a Pschorr cyclization with a more or less controlled regioselectivity which leads to rather moderate yields. The first derivatives published in 2003 did not

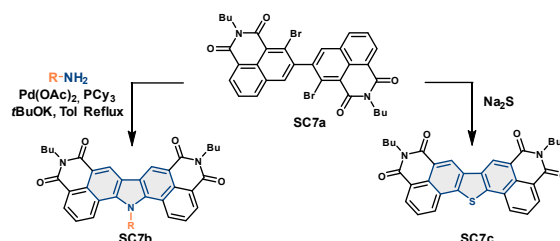
exhibit interesting photophysical properties, but were found good DNA binders and were envisaged for therapeutic applications.<sup>33</sup> In 2007, Liu et al. proposed *N*-oxide derivatives as prodrugs for hypoxic tumors<sup>16a</sup> and in 2013, Xu showed that the activity of these compounds was probably related to the inhibition of topoisomerases I and II.<sup>34</sup> These derivatives were later used as PDT agents by Quian's group.<sup>35</sup> Gellerman then proposed a revised procedure to fuse naphthalimide to a carbazole.<sup>36</sup> The latter ring was formed *via* a regioselective thermal nitrene insertion reaction. The azido precursor of the nitrene being produced through a Suzuki reaction followed by azidation under Sandmeyer conditions. Multiple compounds have been obtained by this route but once again the fluorescence properties have not been described.



<sup>a</sup>  $[\text{c}] = \sim 10^{-4}$  M.  
<sup>b</sup> Absolute quantum yield measured by using an integrating sphere.

**Figure 11.** Dibenzofuran and carbazol/naphthalimide fused hybrid dyes and their photophysical properties. Figure adapted from the literature.<sup>37</sup> Reprinted from Tetrahedron Letters, 52/42, Rui Umeda, Hiroaki Nishida, Motohiro Otono, Yutaka Nishiyama,  $\pi$ -Sufficient heteroaromatic compounds fused naphthalimide unit as novel solvatochromic fluorophores, Pages 5494-5496., Copyright (2011), with permission from Elsevier.

The first real proposal for novel fluorescent compounds was brought by Nishiyama's group.<sup>37</sup> Unlike his predecessors, Nishiyama considered a final palladium-catalyzed intramolecular cyclization to yield benzofuran and carbazole derivatives in reasonable yields. Several derivatives were obtained and their photophysical properties were studied (Figure 11). They show a pronounced solvatochromism independently of the nature of the fused heterocycle. The best properties are obtained for the methoxy derivatives **11c** and **11'c**, suggesting that a donating group at this position producing ICT is beneficial. Also, more donor moieties such as dimethylamino would be interesting.



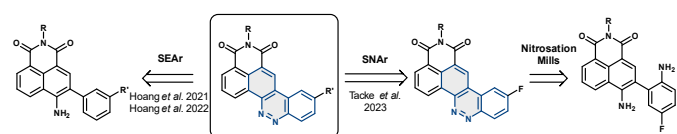
**Scheme 7.** Synthesis of carbazol or dibenzothiophene based A- $\pi$ -A dimers fused hybrid dyes.<sup>38</sup>

Finally, we can mention the work of Liu's group who propose to combine two naphthalimide units on each side of carbazole<sup>38a</sup> or thiophene<sup>38b</sup> unit in order to obtain A- $\pi$ -A derivatives

presented in Scheme 7. The thiophene derivative can be easily oxidized with mCPBA in order to form the corresponding sulfoxide. The photophysical properties of the described compounds are quite common, on the other hand, an optoelectrical characterization, together with DFT calculations, revealed a relatively low level of LUMO which justifies, according to the authors, to consider these new species as serious n-type semiconductor candidates

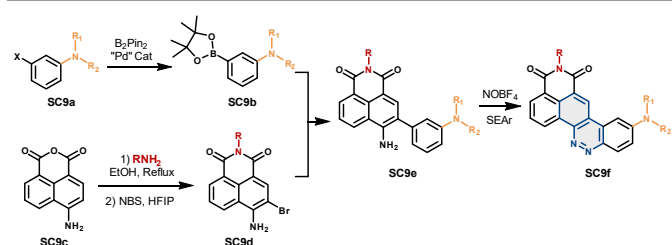
## Cinnoline for access to many red-emitting dyes

Our group has also participated in the development of hybrid fluorophores by fusing a cinnoline unit to naphthalimides.



**Scheme 8.** Synthetic strategies for the access to cinnoline/naphthalimide "CinNapht" dyes.<sup>39</sup>

This was inspired by recent achievements demonstrating that the *in situ* formation of the N=N double bond upon the reaction of aniline derivative with endogenous NO led to fluorescent compounds.<sup>40</sup> However neither the synthesis nor the photophysical study of the presumably formed compounds were reported. For this purpose, we developed two synthetic strategies. The first approach was based on a final intramolecular SEAr step operating on a diazonium salt formed *in situ* from an aniline bisaryl intermediate (Scheme 8, left).<sup>39a</sup> The emission of the so-formed dye was obviously redshifted in comparison with 4-ANI, exhibiting a maximum emission wavelength shifted +89 nm in dichloromethane (DCM). We also noticed a strong solvatochromism with an emission maximum reaching 682 nm in DMSO. DFT and TD-DFT calculations confirmed that the CinNapht fluorescence mechanism was based on an internal charge transfer (ICT) which explained the marked solvatochromism from green to red in the most polar solvents. The first assays demonstrated quite good efficiency for cell imaging, and the dye was found to be nontoxic for the cells. This set of data led us to consider CinNaphts as promising fluorophores. A set of fluorophores was prepared modifying both the nitrogen-substituting group of the naphthalimide unit and the donor part of the fluorophore (Scheme 9).<sup>39b</sup>



**Scheme 9.** Synthetic access to cinnoline/naphthalimide "CinNapht" dyes.<sup>39b</sup>

We were thus able to show that modification of the amine donor resulted in tuning the photophysical properties. Moreover, the introduction of moieties thought to target specific cellular compartments afforded new cellular organelle

markers with large Stoke Shift. Representative examples are presented in Figure 12.

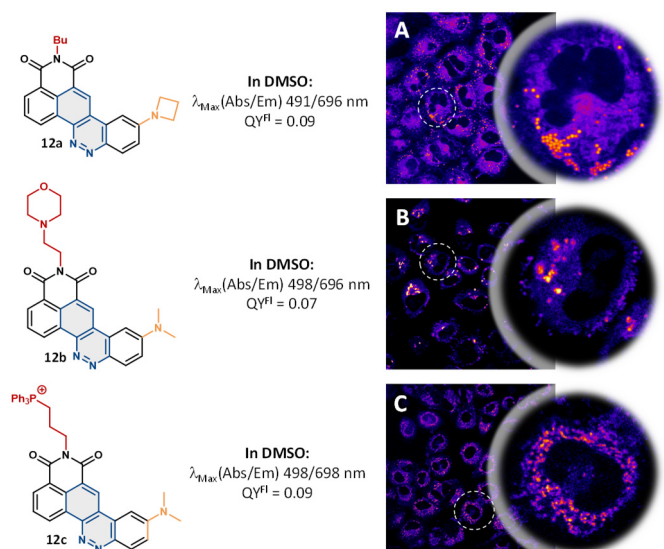
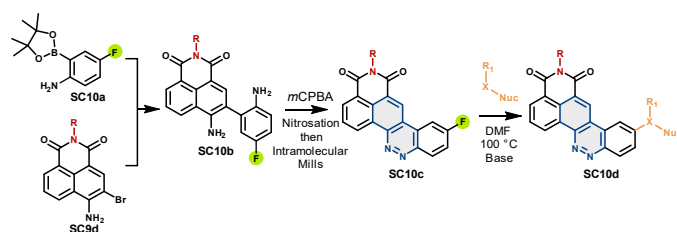


**Figure 12.** Examples of CinNapht dyes obtained with the original synthetic strategy and their use for cell organelles imaging.<sup>39b</sup> © 2022 Wiley-VCH GmbH

This way we made possible the fluorescence imaging of lipid droplets (**12a**), lysosome (**12b**) or mitochondria (**12c**). Considering the promising results obtained with this first set of CinNaphts, we proposed an alternative synthetic route in order to provide easier access to multiple compounds that could offer new perspectives. A strategy of late stage introduction of nucleophilic species by SNAr was thus developed.<sup>39c</sup> It was based on the use of stable and easily accessible aryl fluoride analog of CinNapht. We demonstrated that this strategy permits the introduction of various nucleophiles in good yields.



**Scheme 10.** SNAr late-stage introduction of nucleophiles by SNAr for easy access to "CinNapht" dyes.<sup>39c</sup>

Among the synthesized and described compounds, we can mention bioconjugatable derivatives (carboxylic acid, primary amines, alkynes) or sugar derivatives. Moreover, the introduction of a sulfonated lipophilic amine (**13a**) or an amine derivative of Hoechst (**13b**) provided new selective markers of the plasma membrane (Figure 13, top) and the nucleus (Figure 13, bottom). Finally, a diphenylamine derivative **14** was obtained (Figure 14). It displays a marked AIEE behavior with the capacity to accumulate selectively in lipid droplets thus allowing their imaging in living cells with a particularly high signal-to-noise ratio. Photophysical characterization indicates that the emission spectrum of the dye recorded within the LDs is very close to the one recorded in oil. This set of data

confirmed that CinNapht **14** constitutes a powerful tool for imaging of live cell lipid droplets.

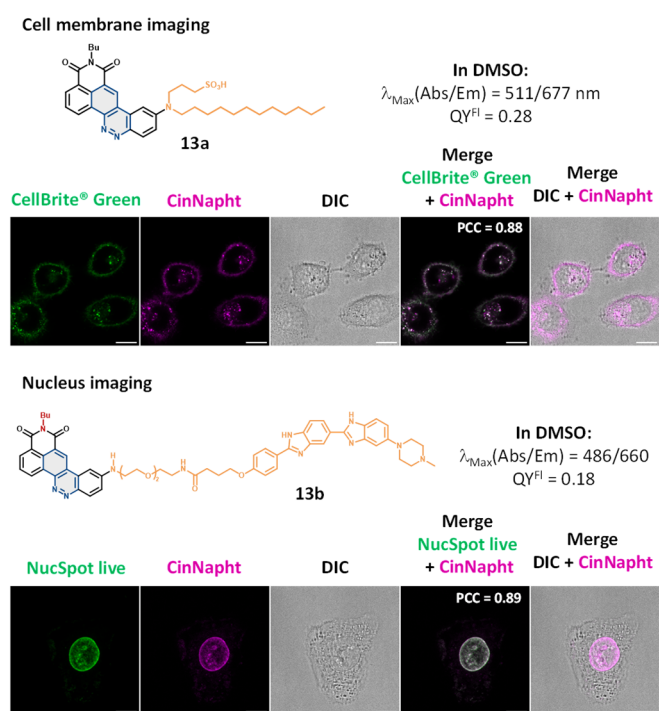


**Figure 13.** Imaging of cell membrane and nucleus and with analogs of CinNaphts obtained by SNAr.<sup>39c</sup>

We also turned our attention to optimizing the photophysical properties of our fluorophores, and in particular to improve their resistance to photobleaching. Recently, the Lavis group demonstrated that the introduction of deuterium atoms in place of hydrogen atoms on the donor amine greatly improved this parameter.<sup>41</sup>

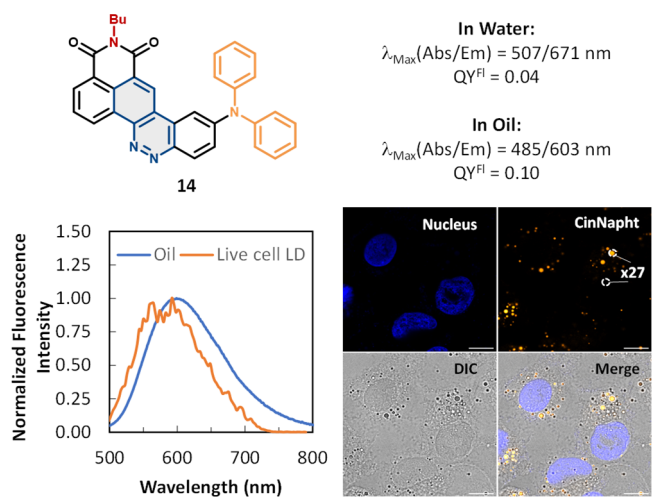


**Figure 14.** A diphenylamine derivative of CinNapht to observe lipid droplets in live cells. Emission spectra recorded in oil and in LD. Imaging of LD in living cells by confocal microscopy.<sup>39c</sup>

Inspired by these results, we prepared a CinNapht analog in which the donating pyrrolidine ring was deuterated in the alpha position. The full photophysical characterization of this analog (**15a**), and comparison with the non-deuterated one (**15b**),

demonstrated the real interest of the deuterium atom in the quest of improving the photobleaching resistance (Figure 15). On the other hand, we could notice that this strategy has no significant effect on other photophysical properties (Absorption and emission wavelengths, fluorescence quantum yield).

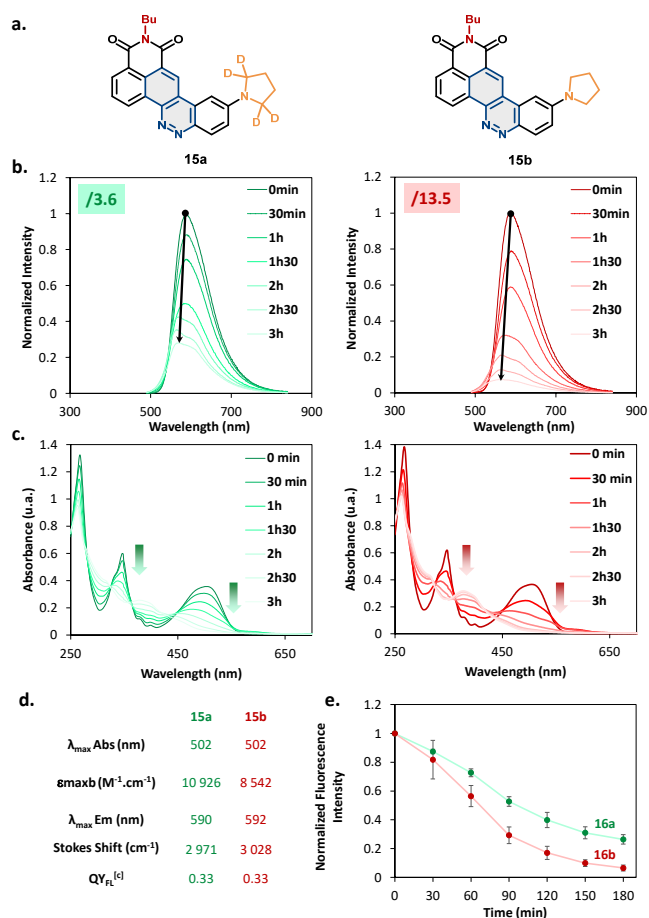


**Figure 15.** Influence of deuteration of pyrrolidine. (a) Structures of deuterated CinNapht **15a** and non-deuterated CinNapht **15b**. (b) Normalized fluorescence spectra of compounds **15a** and **15b** in  $\text{CHCl}_3$  at 25 °C every 30 min over 3 h of irradiation at 470 nm. (c) Absorbance spectra of compounds **15a** and **15b** in  $\text{CHCl}_3$  at 25 °C every 30 min over 3 h of irradiation at 470 nm. (d) Table of comparison of photophysical characteristics of CinNaphts **15a** and **15b**. (e) Comparison of fluorescence intensity decline over time after irradiation at 470 nm.<sup>39c</sup>

These examples demonstrate the benefits of extending the naphthalimide conjugation by fusing a cinnoline moiety to the naphthalimide backbone. To date, CinNaphts have only been proven suitable for imaging cell organelles. We are currently working on new analogs that will offer the opportunity to use CinNaphts as functionalizable platforms for fluorogenic sensing, which I believe is the next logical step in the development of these fused hybrid fluorophores, given the promising results presented above.

## Conclusion and perspectives

In conclusion to this review of fused hybrid fluorophores incorporating the naphthalimide skeleton, we can state that multiple families of heterocycles have already been associated with ANI (Table 1). Although many examples were initially

developed to offer molecules endowed with therapeutic properties, there are now several articles showing the potential of this strategy for the development of new luminescent devices. The field of optoelectronics is particularly well represented, especially by the work of Cabanetos' group. As far as fluorescence imaging is concerned, we notice that when objects are engineered with the aim of generating molecules dedicated to fluorescence imaging, the results are quite convincing. For example, Lin's hemicyanins have led to the development of various fluorogenic probes. There is real potential here in my opinion. The diversification of the aldehyde partners, or the use of hybrids fused to ANI/benzoxazoles and

ANI/benzothiazol can constitute promising lines of thought to be considered for the preparation of new optical imaging tools. Our work has also demonstrated real utility in this field, particularly by allowing the imaging of cell organelles in living cells with wide Stokes Shift fluorophores called CinNaphts. The next step will be to use them to design responsive sensors and bring them in the field of fluorogenic detection. Generally speaking, we can only regret that there aren't more examples associating a donor group with hybrid backbones in order to establish an internal charge transfer favorable to fluorescence. This is probably one of the most promising avenues of investigation for hybrid molecules.

**Table 1.** Compilation of the dyes mentioned in this review with their photophysical properties and uses.

Heterocycle fused to ANI	molecule	Abs/Em (nm)	QY <sub>FL</sub>	QY <sub>FL</sub> solid	QY <sub>Δ</sub>	epsilon	Solvent	Application	Ref
Thioxanthene	<b>1</b>	395/523	-	-	-		Acetone	Ceramic impregnation	7
	<b>D1</b>	455/502	0.19	0.06	-	51 000	CH <sub>2</sub> Cl <sub>2</sub>	OLED	8
	<b>D2</b>	384/509	0.29	0.14	-	37 000	CH <sub>2</sub> Cl <sub>2</sub>	OLED	8
	<b>D3</b>	473/530	0.34	0.18	-	31 000	CH <sub>2</sub> Cl <sub>2</sub>	OLED	8
	<b>TCI<sub>2</sub></b>	489/523	0.20		-	33 500	CH <sub>2</sub> Cl <sub>2</sub>	Flexible OLED	12
	<b>4a</b>	459/600	0.01		0.75	23 200	DMSO	Photosensitizers - PDT	13
	<b>4b</b>	460/601	0.01	-	0.82	16 600	DMSO	Photosensitizers - PDT	13
	<b>4c</b>	457/585	0.013	-	-	10 800	DMSO	Photosensitizers - PDT	13
Xanthène	<b>O-Xant-5</b>	448/460	-	-	-	25 500	EtOAc		16
	<b>O-Xant-8</b>	449/506	-	-	-	18 500	EtOAc		16
	<b>O-Xant-9</b>	457/491	-	-	-	16 700	EtOAc	phosphor LED systems	16
	<b>O-Xant-10</b>	455/489	-	-	-	15 600	EtOAc		16
	<b>O-Xant-11</b>	450/499	-	-	-	19 000	EtOAc		16
Merocyanines trough indole-fused hybride	<b>TPFC-1</b>	376/443	0.37	-	-	13 060	PBS buffer	Two photons imaging (cells and brain slices)	20
	<b>TPFC-2</b>	418/537	0.11	-	-	14 580	PBS buffer		20
	<b>TPFC-3</b>	428/594	0.22	-	-	13 620	PBS buffer		20
	<b>TPFC-4</b>	452/611	0.12	-	-	16 120	PBS buffer		20
	<b>TPFC-5</b>	492/669	0.10	-	-	25 220	PBS buffer		20
	<b>TPFC-Lyso-1</b>						PBS buffer	Two photons imaging of lysosome	20
	<b>TPFC-Lyso-2</b>						PBS buffer		20
	<b>TPFC-Lyso-3</b>						PBS buffer		20
	<b>TPFC-Lyso-4</b>						PBS buffer		20
	<b>TPFC-Lyso-5</b>						PBS buffer		20
	<b>7a</b>	Responsive OFF-ON probe derived from <b>TPFC-4</b>						PhSH responsive	21
	<b>7b</b>	Responsive OFF-ON probe derived from <b>TPFC-4</b>						GSH/Cys responsive	22
	<b>7c</b>	Responsive OFF-ON probe derived from <b>TPFC-5</b>						Fe <sup>2+</sup> responsive	23
Cyanines through indole-fused hybride	<b>ML880</b>	880/912	0.11	-	-	88 390	DMSO	PDT/PTT	24
		936/-	-	-	-	58 000	PBS buffer	Chemotherapy when associated with drug	
benzimidazolone	<b>9a</b>	436/559	0.02	-	-			<b>9'a</b> resulting from activation of <b>9a</b> by phosgène	28
	<b>9'a</b>	411/468	0.59	-	-				28
benzimidazole	<b>9b</b>		< 0.01					<b>9'b</b> resulting from activation of <b>9b</b> by phosgène	29
	<b>9'b</b>	380 <sup>a</sup> /450 <sup>a</sup>	0.23	-	-		PBS buffer		29
	<b>10a</b>	375/-	-	-	-		dioxane	<b>10a</b> is used as a "OR" responsive probe to detect phosgene ( <b>10b</b> ) or triphosgene ( <b>10c</b> )	31
	<b>10b</b>	390 <sup>a</sup> /422	-	-	-		dioxane		31
<b>10c</b>	435 <sup>a</sup> /526	-	-	-		dioxane	31		
carbazole	<b>11a</b>	398/467	0.65	-	-	13 000	CH <sub>2</sub> Cl <sub>2</sub>	Study of photophysical properties in solution	37
	<b>11b</b>	382/446	0.74	-	-	15 200	CH <sub>2</sub> Cl <sub>2</sub>		37
	<b>11c</b>	409/514	0.25	-	-	14 100	CH <sub>2</sub> Cl <sub>2</sub>		Solvatochromism
dibenzofuran	<b>11'a</b>	382/416	0.31	-	-	8 600	CH <sub>2</sub> Cl <sub>2</sub>	Study of photophysical properties in solution	37
	<b>11'b</b>	376/407	0.27	-	-	8 600	CH <sub>2</sub> Cl <sub>2</sub>		37
	<b>11'c</b>	361/494	0.15	-	-	12 200	CH <sub>2</sub> Cl <sub>2</sub>		Solvatochromism
Cinnoline	<b>12a</b>	491/696	0.09	-	-	12 939	DMSO	Lipid droplet imaging	39b
	<b>12b</b>	498/696	0.07	-	-	14 032	DMSO	Lysosome imaging	39b
	<b>12c</b>	498/698	0.09	-	-	11 912	DMSO	Mitochondria imaging	39b
	<b>13a</b>	511/677	0.28	-	-	4 639	DMSO	Plasma membrane imaging	39c
	<b>13b</b>	486/660	0.18	-	-	4 763	DMSO	Nucleus imaging	39c
	<b>14</b>	507/671	0.04	-	-	11 313	H <sub>2</sub> O	AIEE/ Lipid droplet imaging	39c
	485/603	0.10	-	-	13 255	Oil			

<b>15a</b>	502/690	0.33	-	-	10 926	CHCl <sub>3</sub>	Photobleaching resistance study	39c
<b>15b</b>	502/592	0.33	-	-	8 542	CHCl <sub>3</sub>	Photobleaching resistance study	39c

<sup>a</sup>Estimated value based on spectra observations (no explicit value being accessible in the reference publication).

## Conflicts of interest

There are no conflicts to declare.

## Acknowledgements

I thank the University Paris-Saclay the CNRS and Institut de Chimie des Substances Naturelles for their financial support. A special thank to students who worked on the CinNapht project (Dr. Minh-Duc HOANG and Ms. Eléonore TACKE) and to Dr. Philippe DURAND for proofreading and suggestions before submission of this manuscript.

## Notes and references

- D. Gudeika, *Synth. Met.*, 2020, **262**, 116328.
- a) H.-Q. Dong, T.-B. Wei, X.-Q. Ma, Q.-Y. Yang, Y.-F. Zhang, Y.-J. Sun, B.-B. Shi, H. Yao, Y.-M. Zhang and Q. Lin, *J. Mat. Chem. C*, 2020, **8**, 13501;b) N. Jain and N. Kaur, *Coord. Chem. Rev.*, 2022, **459**, 214454;c) C. Geraghty, C. Wynne and R. B. P. Elmes, *Coord. Chem. Rev.*, 2021, **437**, 213713;d) H. Yu, Y. Guo, W. Zhu, K. Havener and X. Zheng, *Coord. Chem. Rev.*, 2021, **444**, 214019.
- a) F. Würthner, C. R. Saha-Möller, B. Fimmel, S. Ogi, P. Leowanawat and D. Schmidt, *Chem. Rev.*, 2016, **116**, 962;b) M. Sun, K. Müllen and M. Yin, *Chem. Soc. Rev.*, 2016, **45**, 1513;c) P. Singh, P. Sharma, N. Kaur, L. S. Mittal and K. Kumar, *Anal. Methods*, 2020, **12**, 3560.
- a) M. Al Kobaisi, S. V. Bhosale, K. Latham, A. M. Raynor and S. V. Bhosale, *Chem. Rev.*, 2016, **116**, 11685;b) S. V. Bhosale, C. H. Jani and S. J. Langford, *Chem. Soc. Rev.*, 2008, **37**, 331.
- a) J. J. Li, Pschorr cyclization, in *Name Reactions: A Collection of Detailed Mechanisms and Synthetic Applications*, Springer Berlin Heidelberg, 2009, 450;b) R. Pschorr, *Berichte der deutschen chemischen Gesellschaft*, 1896, **29**, 496.
- J. P. S. Farinha, M. A. Winnik and K. G. Hahn, *Langmuir*, 1999, **15**, 7088.
- B. J. Crosby, J. Unsworth and F. W. D. Rost, *Journal of Microscopy*, 1996, **181**, 61.
- P. Josse, S. Li, S. Dayneko, D. Joly, A. Labrunie, S. Dabos-Seignon, M. Allain, B. Siegler, R. Demadrille, G. C. Welch, C. Risko, P. Blanchard and C. Cabanetos, *J. Mat. Chem. C*, 2018, **6**, 761.
- J. M. Andrés Castán, L. Abad Galán, S. Li, C. Dalinot, P. Simón Marqués, M. Allain, C. Risko, C. Monnerneau, O. Maury, P. Blanchard and C. Cabanetos, *New J. Chem.*, 2020, **44**, 900.
- J. M. Andres Castan, C. Dalinot, S. Dayneko, L. Abad Galan, P. Simon Marques, O. Aleveque, M. Allain, O. Maury, L. Favereau, P. Blanchard, G. C. Welch and C. Cabanetos, *Chem. Commun.*, 2020, **56**, 10131.
- P. Josse, K. Morice, D. Puchán Sánchez, T. Ghanem, J. Boixel, P. Blanchard and C. Cabanetos, *New J. Chem.*, 2022, **46**, 8393.
- J. M. A. Castán, C. Amruth, P. Josse, L. A. Galan, P. S. Marqués, M. Allain, O. Maury, T. Le Bahers, P. Blanchard, C. Monnerneau, G. C. Welch and C. Cabanetos, *Mat. Chem. Front.*, 2022, **6**, 1912.
- L. Zhang, Z. Huang, D. Dai, Y. Xiao, K. Lei, S. Tan, J. Cheng, Y. Xu, J. Liu and X. Qian, *Org. Lett.*, 2016, **18**, 5664.
- M. Deiana, P. Josse, C. Dalinot, A. Osmolovskiy, P. S. Marques, J. M. A. Castan, L. Abad Galan, M. Allain, L. Khrouz, O. Maury, T. Le Bahers, P. Blanchard, S. Dabos-Seignon, C. Monnerneau, N. Sabouri and C. Cabanetos, *Chem. Commun.*, 2022, **5**, 142.
- A. T. Peters and Y. S. S. Behesti, *J. Soc. Dye. Colour.*, 2008, **105**, 29.
- a) H. Yin, Y. Xu, X. Qian, Y. Li and J. Liu, *Bioorg. Med. Chem. Lett.*, 2007, **17**, 2166;b) H. Yin, W. Zhu, Y. Xu, M. Dai, X. Qian, Y. Li and J. Liu, *Eur. J. Med. Chem.*, 2011, **46**, 3030.
- J. Lub, S. L. J. Hamon, P. A. van Hal, T. J. Visser, J. M. Jansen and R. A. M. Hikmet, *Dyes and Pigm.*, 2018, **149**, 662.
- L. W. Shen, M. Q. Qian, K. Yu, S. Narva, F. Yu, Y. L. Wu and W. Zhang, *Sci. Rep.*, 2020, **10**, 7635.
- Z. Tian, Y. Liu, B. Tian and J. Zhang, *Res. Chem. Intermed.*, 2013, **41**, 1157.
- H. Chen, Y. Tang, H. Shang, X. Kong, R. Guo and W. Lin, *J. Mater. Chem. B*, 2017, **5**, 2436.
- L. Huang, Y. Chen, Y. Zhao, Y. Wang, J. Xiong, J. Zhang, X. Wu and Y. Zhou, *Chin. Chem. Lett.*, 2020, **31**, 2941.
- S. Zhou, Y. Rong, H. Wang, X. Liu, L. Wei and X. Song, *Sens. Actuators B: Chem.*, 2018, **276**, 136.
- Y. Rong, C. Wang, P. Chuai, Y. Song, S. Zhou, P. Hou, X. Liu, L. Wei and X. Song, *New J. Chem.*, 2019, **43**, 13212.
- T. Jin, D. Cheng, G. Jiang, W. Xing, P. Liu, B. Wang, W. Zhu, H. Sun, Z. Sun, Y. Xu and X. Qian, *Bioact. Mater.*, 2022, **14**, 42.
- a) W. Yao and X. Qian, *J. Fluor. Chem.*, 2000, **106**, 69;b) W. Yao, X. Qian and Q. Hu, *Tet. Lett.*, 2000, **41**, 7711.
- X. Qian, Z. Li and Q. Yang, *Bioorg. Med. Chem.*, 2007, **15**, 6846.
- A. Botz, Y. Chenavier, J. Pécaut, P. Delangle and C. Gateau, *Tet. Lett.*, 2018, **59**, 2550.
- S. L. Wang, L. Zhong and Q. H. Song, *Chem. Eur. J.*, 2018, **24**, 5652.
- S. Cai, C. Liu, X. Jiao, L. Zhao and X. Zeng, *Tetrahedron*, 2020, **76**.
- J. Tan, Z. Li, Z. Lu, R. Chang, Z. Sun and J. You, *Dyes and Pigm.*, 2021, **193**, 109540.
- S. L. Wang, C. Li and Q. H. Song, *Anal. Chem.*, 2019, **91**, 5690.
- a) A. Romieu, *Org. Biomol. Chem.*, 2015, **13**, 1294;b) S. Erbas-Cakmak, S. Kolemen, A. C. Sedgwick, T. Gunnlaugsson, T. D. James, J. Yoon and E. U. Akkaya, *Chem. Soc. Rev.*, 2018, **47**, 2228.
- Y. Xu, X. Qian, W. Yao, P. Mao and J. Cui, *Bioorg. Med. Chem.*, 2003, **11**, 5427.
- S. Tan, H. Yin, Z. Chen, X. Qian and Y. Xu, *Eur. J. Med. Chem.*, 2013, **62**, 130.
- L. Zhang, K. Lei, J. Zhang, W. Song, Y. Zheng, S. Tan, Y. Gao, Y. Xu, J. Liu and X. Qian, *Med. Chem. Comm.*, 2016, **7**, 1171.
- A. Rozovsky, E. Regozin, M. Oron-Herman, A. Albeck and G. Gellerman, *Eur. J. Chem.*, 2015, **2015**, 1811.
- R. Umeda, H. Nishida, M. Otono and Y. Nishiyama, *Tet. Lett.*, 2011, **52**, 5494.
- a) D. Wu, Y. Zhang, J. Zhang, S. H. Liu and J. Yin, *Chem. Asian J.*, 2015, **10**, 1344;b) D. Wu, Z. Chen, Y. Zhang, J. Zhang, S. H. Liu and J. Yin, *J. Org. Chem.*, 2015, **80**, 8443.
- a) M.-D. Hoang, J.-B. Bodin, F. Savina, V. Steinmetz, J. Bignon, P. Durand, G. Clavier, R. Meallet-Renault and A. Chevalier, *RSC Adv.*, 2021, **11**, 30088;b) M.-D. Hoang, F. Savina, P. Durand, P. R. Meallet-

Renault, G. Clavier and A. Chevalier, *ChemPhotoChem*, 2022, **6**, e202200138;c) E. Tacke, M.-D. Hoang, K. Tatoueix, B. Keromnes, E. Van Eslande, P. Durand, G. Pieters and A. Chevalier, *Chem. Sci.*, 2023.  
40. a) H. Zhang, X. Zhu and Y. Wang, **2017**;b) X. Zhu, J. Q. Chen, C. Ma, X. Liu, X. P. Cao and H. Zhang, *Analyst*, 2017, **142**, 4623.  
41. J. B. Grimm, L. Xie, J. C. Casler, R. Patel, A. N. Tkachuk, N. Falco, H. Choi, J. Lippincott-Schwartz, T. A. Brown, B. S. Glick, Z. Liu and L. D. Lavis, *JACS Au*, 2021, **1**, 690.